Case Studies in Thermal Engineering 52 (2023) 103718

Contents lists available at ScienceDirect

Case Studies in Thermal Engineering

journal homepage: www.elsevier.com/locate/csite

Multipurpose optimization of fuel injection parameters for diesel engine using response surface methodology

Muhammad Usman [a,*], Muhammad Kashif Tariq [a], Muhammad Ali Ijaz Malik [b], Fahid Riaz [c,**], Bashar Shboul [d], Muhammad Usman [a], Yasser Fouad [e], Muhammad Imran Masood [f]

[a] Department of Mechanical Engineering, University of Engineering and Technology, Lahore, 54890, Pakistan
[b] Department of Mechanical Engineering, Superior University, Raiwind Road, Lahore, Pakistan
[c] Mechanical Engineering Department, Abu Dhabi University, Abu Dhabi, P.O. Box 59911, United Arab Emirates
[d] Renewable Energy Engineering Department, Faculty of Engineering, Al Al-Bayt University, Mafraq, Jordan
[e] College of Applied Mechanical Engineering, College of Applied Engineering, Muzahimiyah Branch, King Saud University, P.O. Box 800, Riyadh 11421, Saudi Arabia
[f] Department of Engineering and Aviation UHI Perth, Crieff Road, Perth, PH1 2NX, UK

HIGHLIGHTS

- The effect of fuel injection nozzle is ascertained for engine operation.
- The effect of nozzle protrusion is studied for engine operation.
- Optimization of system reveals a composite desirability of 0.712.
- The effective nozzle pressure appears as 240 bar at a protrusion of 2.5 mm.

GRAPHICAL ABSTRACT

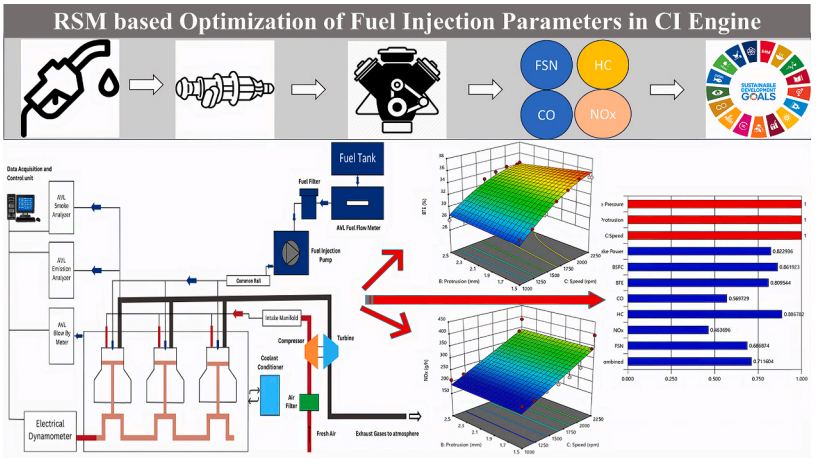

* Corresponding author.
** Corresponding author.
E-mail addresses: muhammadusman@uet.edu.pk (M. Usman), fahid.riaz@adu.ac.ae (F. Riaz).

https://doi.org/10.1016/j.csite.2023.103718
Received 20 July 2023; Received in revised form 17 October 2023; Accepted 2 November 2023
Available online 4 November 2023
2214-157X/© 2023 The Authors. Published by Elsevier Ltd. This is an open access article under the CC BY-NC-ND license (http://creativecommons.org/licenses/by-nc-nd/4.0/).

ARTICLE INFO

Handling Editor: Huihe Qiu

Keywords:
Fuel injection parameters
Diesel engine
Optimization
Filter smoke number
Desirability

ABSTRACT

The hike in fuel prices and rapid depletion of fuel reserves have compelled scientists to focus on energy conservation, environmental protection, engine performance improvement, and cost saving. The prime objective of the study is to compare the empirical results with response surface methodology (RSM) optimized results in order to check the accuracy of model designed by RSM. Therefore, the current study examines the effect of fuel injection parameters (nozzle opening pressure and protrusion) on diesel engine performance and exhaust emissions. RSM technique was applied to predict engine performance and exhaust emission parameters along with their optimization. The brake thermal efficiency (BTE) was incremented by 1.23 % for protrusion from 1.5 to 2.5 mm under 240 bar nozzle opening pressure (NOP). BTE was increased by 0.94 and 4.51 % for 1.5 and 2.5 mm protrusion respectively. CO emission was decremented by 4.47 and 11.31 % for 1.5 and 2.5 mm protrusion respectively when the NOP changed from 230 to 240 bar. RSM model optimized input conditions 240 bar pressure, 2.5 mm protrusion, and 1935.67 engine rpm. The engine was again tested on RSM-optimized conditions and the highest absolute percentage error (APE) of 4.42 % was obtained for NOx emission, while the lowest APE of 2.89 % was obtained for BSFC.

1. Introduction

Compression Ignition (CI) engines have potentially contributed to socio-economic growth due to their inclusive range of applications in agriculture, transportation, industries, and power generation [1,2]. The transportation sector solely consumes around 33 % of global energy and served as primary source of pollution in the environment like the global warming, greenhouse effect, acid rains, and smog [3,4]. Fossil fuels served as the primary fuel to power diesel engines, but their immense utilization results in their depletion in approximately the next 50 years [5]. Energy Information Administration (EIA) has projected that global energy consumption will be upsurged by 56 % in 2040 in comparison with 2010 [6]. Therefore, the environmental threats, increase in fossil fuel demand, and their depletion in the near future are forcing engineers to make progress in efficient technology [7]. During the last couple of decades, the automotive sector has paid attention on the improvement of advanced technologies related to emission control due to the escalating dynamic market trends for successfully reducing the emission problems along with better fuel economy. It is important to have an atmosphere within environmental standards for industries. For this purpose, different manufacturers and engineers are making their efforts to advance distinct strategies in operations for a reduction in exhaust emission of petrol as well as diesel engine. Moreover, automotive manufacturers have imposed strict standards related to emissions to make advanced engine models comply with them. A detailed review of the literature reveals three conventional methods for the improvement in engine performance; (i) fuel preprocessing [8,9] (ii) improvement in engine design [10,11] (iii) post-processing of engine exhaust [12]. In fuel preprocessing, the combustion attributes of conventional fuels can be amended by fusing minute fractions of nanoparticles, emulsions, biogas, and biodiesel etc. in petroleum fuel [3,13–15]. The engine design can be improved through a fuel injection system and combustion chamber modification in order to achieve better performance [16–18]. The processing of engine exhaust includes the mitigation of hazardous pollutants in the emissions through catalytic convertors and recirculating them through the engine for better performance [19,20].

The design of combustion chamber and injection nozzle are the two important parameters to decrease exhaust emission along with improved fuel economy. The spray pattern developed by diesel fuel injector has a significant impact on engine performance. Intermittent fuel spray formed under high temperature and pressure usually possess higher turbulence and momentum, which lead to good spray formation in engine cylinder [21]. The geometrical parameters of injector nozzle have been reported to affect the transient behavior of fuel spray jet formation for various conditions of pressures such as needle opening, ambient pressure and injection pressure [22–24]. Also, the spray patterns are directly influenced by different parameters for example the spray orifices and cone angles with their shape, length and diameter, the particular position of the fuel injector with respect to piston forming combustion chamber and lift of needle. The formation of spray jet as well as its impingement depends on these designed variables which show their direct effect on exhaust of engine. The number of spray orifices that forms a jet is very important as for as air fuel mixture is concerned. There exists a direct relation between homogeneity of fuel-air mixture and number of orifices. The combustion process during such condition will produce less exhaust emission [25,26]. Pandian et al. [27] varied injection timing (IT) from 18 to 30° BTDC and found reduction in HC and CO at the cost of higher NOx emission. They observed that BTE improved along with lower HC and CO along with higher NOx emission for upsurge in injection pressure (IP). Also, it is identified that higher injection pressure for moderate protrusion generated better results in terms of higher BTE, lower BSFC, CO and HC emissions.

Agarwal et al. [28] conducted experiment on 510.7 cc CI engine under two distinct fuel injection pressures (1000 and 500 bars) and injection timings. The pressure variations and heat release rate showed better combustion characteristics under lower pressure of 500 bars, however higher-pressure of 1000 bars resulted knocking. The higher combustion and heat release rate was observed for advances injection timings even at earlier combustion stage. The engine performance was improved at lower injection pressure resulting into higher BTE for all engine loading conditions. The performance and emission parameters can be further improved through advancement in the injection timing. The concentration of particulates reduced significantly for higher injection pressure under all loading conditions. It can be credited to prolonged air-fuel mixing time before combustion stroke under advanced injection timings. However, the particulate concentration first rises than decline with retarding injection timing under lower injection pressure due to more sensitive nature of mixing towards cylinder temperature and pressure before combustion stroke.

Hawi et al. [29] found that for 50–150 MPa injection pressure, the vapor penetration increase up to 21.5, 24.4 and 33.2 % for tetradecane, methyl oleate and diesel respectively. For density from 15 to 25 kg/m^3, the wider spray cone angle increases by 11.8, 13.8 and 9.6 % for tetradecane, methyl oleate and diesel respectively. While shorter vapor penetration increases by 11, 9.2 and 13.1 % respectively. They found least reduction in spray cone angle for higher injection pressure. Kushwaha and Ismail [30] performed experiment on 553 cc diesel engine by employing two fuels (HHO gas and diesel fuel) and studied their performance by varying fuel injection parameters. They found that the increase in tip penetration length increased the BTE, decreased BSFC, decline in HC, CO and CO_2, but the NOx emission increased.

RSM comprised of statistical and mathematical methods which are valuable for problem analysis in which response is influenced by multiple factors. It provides multi objective optimization of all the responses influenced by multiple factors [31].

Chaurasia et al. [32] investigated the impact of variable injection timing from 17.5 to 29.5° on diesel engine performance. They observed the increase in fuel consumption from 17.5 to 26.5° and decrease slightly at 29.5°. The opposite trend was observed for brake thermal efficiency. Moreover, the exhaust gas temperature (EGT) decreases with the increase in injection timing because at early injection, more amount of fuel burns in the premixed combustion period which result into higher combustion in-cylinder temperature. The cylinder pressure was increased and ignition delay was decreased when injection timing increased. In case of emissions, CO_2 and NOx were increased with the increase in injection timing, but smoke emissions were decreased. Rajak et al. [33] examined the impact of compression ratio on engine performance. They found that increasing the compression ratio (CR) improved the performance of the engine in terms of peak cylinder pressure, combustion temperature, knocking tendency, NO_X emission and a reduction in brake mean effective pressure, volumetric efficiency, and smoke emission.

Verma et al. [34] characterized the roselle fuel blends, researchers used experimental and empirical approaches while operating at engine loads of 25, 50, 75, and 100 %, and with fuel injection timings of 19°, 21°, 23°, 25°, and 27° before top dead center. Results indicate that for 20 % blend with the change of injection timing from 19° bTDC to 27° bTDC at full load, brake specific fuel consumption and exhaust gas temperature was increased by 15.84 % and 4.60 % respectively, while brake thermal efficiency decreases by 4.4 %. Also, an 18.89 % reduction in smoke, 5.26 % increase in CO2, and 12.94 % increase in NOx were observed. In addition, an empirical model for full range characterization was created. With an r-squared value of 0.9980 ± 0.0011, the artificial neural network model constructed to characterize all 10 variables was able to predict satisfactorily. With improved FIT, Blend LA20 showed greater EGT, ignition delay, and maximum rate of pressure rise. with improved FIT, NOx emissions increased. With enhanced FIT, CO_2 emissions increased while smoke emissions dropped. Rajak et al. [35] studied the impact of load on spray tip penetration and spray cone angle with the increase in load. Both of these parameters were increased with the increase in load. They also observed that B20 biodiesel possessed highest spray tip penetration and lower spray cone angle.

RSM is an efficient and cost-effective tool that not only provides comparison between the predicted and experimental results but also enables us to analyze the experimental factors [36]. Moreover, it optimizes the experimental data which results in saving of the time and resources [37]. The current RSM technique has been used by many scientists for engine performance optimization [38].

Table 1
Comparison between previous research and current study.

Author	Operating Parameters	Output parameters		Combustion parameters	RSM
		Engine performance	Engine emissions		
Yang et al. [41]	Nozzle opening pressures and injection timings	BTE, BSFC	NOx, CO, and HC	ICP, HRR	×
Khayum and Murugan [42]	Nozzle opening pressures, biogas flow rate and injection timings	BTE, BSFC and EGT	NO, CO, HC and smoke	ICP, HRR, ID and combustion duration	×
Khayum et al. [23]	Nozzle opening pressure	BTE, BSFC and EGT	HC, NO and smoke	cylinder pressure	×
Gulmez and Nuran [43]	Nozzle opening pressure and injection timings	Torque, EGT and BTE	SO2, CO2, CO and NOX	×	×
Soudagar et al. [44]	Injection timings and injection opening pressure	BTE, BSFC	CO, HC and NOx	ICP, HRR,	×
Molina et al. [45]	Injection timings	ISFC	Soot, CO, HC and NOx	Start of Combustion, Combustion Duration, Combustion phase, In cylinder pressure	×
Sharma et al. [46]	Injection timings and injection opening pressure	BTE, EGT	×	Peak combustion pressure	✓
Karthic et al. [47]	Injection timings and injection pressure	BTE, BSFC	Smoke, CO, HC and NOx	Ignition delay, In cylinder pressure, HRR	×
Mohamed et al. [48]	Palm biodiesel blend, torque, injection pressure, compression ratio, and injection timing.	BSFC	Smoke, CO	×	✓
Sathiyamoorthi [49]	Injection pressure, and injection timing	BTE, BSFC	Smoke, CO, HC and NOx	×	✓
Sathiyamoorthi [50]	EGR%, Injection pressure, and injection timing	BTE, BSFC	Smoke, CO, HC and NOx	×	✓
Current Study	Nozzle opening pressure, protrusion and engine speed	Brake power, BSFC, BTE	FSN, CO, HC and NOx	×	✓

Samet uslu [39] used different biodiesel blends in CI engine for its performance optimization. He found more optimized results for RSM as compared to Artificial Neural Network (ANN) technique. The R^2 values by RSM model was above 0.90, however, the R^2 values by ANN model were in range of 0.88–0.95. However, the mean relative error (MRE) and root mean square error (RMSE) in case of all responses were found lower. The optimum responses were identified as 0.126 %, 196.25 ppm, 155.49 °C, 0.126 %, 69.11 %, 30.75 % for HC, NOx, EGT, CO, smoke and BTE for optimum operating factors (17.88 % palm oil percentage, 780-W engine load and 35 °CA injection advance). Baranitharan et al. [40] compared RSM and ANN techniques for the evaluation and optimization of engine factors for ternary (biodiesel/diesel/*tert*-butyl hydroxyl quinone) fuel blends. The study was conducted under different engine loads and compression ratios. The RSM optimized values were 22.01 % BTE, 8.33 % CO_2, 9.33kg/kWh BSFC, 0.67 % CO, 224 ppm HC and 351 ppm NOx emissions. Moreover, the R^2 values for RSM and ANN were found 0.991 and 0.998 respectively. Usman et al. conducted experiment on hydroxy gas (HHO) enriched diesel fuel and optimized the diesel engine performance through RSM. Analysis of variance (ANOVA) results depicted good fit for all developed quadratic models. The user-defined historical RSM design of empirical study recognized optimum HHO flow rate (8 L/min) and engine load (41 %), with 0.733 composite desirability and absolute percentage error (APE) below 5 %. The literature review discloses that RSM has been considerably applied to optimize CI engine performance for alternative fuels.

1.1. Novelty

Table 1 entails the comparison between literature review and the current study. It can be observed that the most of research does not include the application of response surface methodology (RSM) for the optimization of engine performance. Only few researchers used RSM approach for engine performance optimization, but they do not include all engine performance and emission parameters. They mostly include combustion parameters of engine, but these parameters automatically reflect through engine brake power, fuel consumption, engine efficiency and emissions. For better combustion, engine will produce higher brake power at the cost of lower fuel consumption and efficiency. The engine performance will be compromised for the worst combustion. Two aspects have been noticed after reviewing the literature. One is that the researcher applied RSM only for optimization engine performance but did not validate the RSM results, and ANOVA is also missing in the literature. Secondly, it is noticed that researchers applied RSM for limited engine performance parameters. In present study, injection timing is not changed and there is no relative relation of injection timing with compression pressure. However, the distance of injectors relative to the piston is increased by placing different thickness of washer at the protrusion where injector has to be seated. This change has varied the time for fuel to reach the piston cavity. The very change is done to see its impact on the performance and emissions which has not been given attention in the literature. Further, this study focuses on RSM application on fuel injection parameters of diesel engine due to its benefits over machine learning optimizations. As RSM can deal with nonlinear relationship among variable, multi objective optimization, quantify the importance of input and output variable along with statistical assessment of optimized results. Moreover, RSM requires fewer experiments for than other optimization techniques, which can save time and resources. RSM achieves this by using a combination of design of experiments and statistical models to generate predictions for untested input conditions. RSM is multi objective optimization that include all input parameters (protrusion, nozzle opening pressure and engine speed) and response variable (Brake power, BSFC, BTE, FSN, CO, HC and NOx). ANOVA analysis has been made on the performance and emission parameters against input factors (protrusion, nozzle pressure and engine speed). At last, the RSM predicted optimized results were validated via experimentation.

2. Materials and methodology

In the current study, turbo charged diesel engine was used and fuel injection parameters were varied to ascertain emission and performance characteristics. The technical specification of engine and physicochemical properties of diesel fuel are mentioned in Table 2 and Table 3 respectively.

2.1. Experimental setup

A three-cylinder, water cooled, 2.5-L diesel engine (model: MF 260) was retrofitted with eddy current dynamometer. The dynamometer was mounted on inflexible base plate which takes shaft rotor assemblage inside metal casing. The engine shaft coupled with engine rotor and rotates with crankshaft in order to synchronize with engine speed cutting magnetic lines. In consequence, the eddy currents will be produced which opposes direction of shaft in clockwise direction. This opposition by eddy current actually served as electric load and dissipates heat. The cooling water regularly circulates through pipes to reduce heat dissipation impact. The engine rpm is measured by electro-magnetic pick-up device fixed on toothed wheel. The probe of exhaust gas analyzer (NOVA 7466LK) was

Table 2
Engine specification.

Parameters	Specification
Engine capacity	2.5 L
Engine make	AD3.1524 by Perkins
Bore	91.44 mm
Stroke	127 mm
Compression ratio	16.5
Maximum Torque	171N-m
Maximum Power	34.6 kW

Table 3
Fuel properties.

Properties	Diesel	ASTM standards
Physical state	Liquid	
(Specific gravity) $_{16°C}$	0.83–0.86	ASTM D1298
Stoichiometric Air to fuel ratio	14.5	–
(Viscosity)$_{40°C}$	2.42 mm^2/s	ASTM D445
Boiling Range	160–366 °C	ASTM D2887
Cetane rating	57.86	ASTM D613
Flash point	59 °C	ASTM D92
Calorific value	44000 kJ/kg	ASTM D240

inserted into exhaust manifold of engine in order to record steady state emissions. Fig. 1 displays the experimental setup including test engine and all auxiliaries attached with it.

A smoke meter manufactured by the "AVL" was used in the experimentation in order to ascertain smoke value. The AVL smoke meter determines the filter smoke number (FSN) and soot concentration by using the filter paper method. The AVL smoke meter provides high measurement resolution and low detection limit of 0.001 FSN and 0.002 FSN respectively.

The primary purpose of the research study is to achieve the combination of design parameters (nozzle opening pressure, protrusion and engine speed) which should be suitable for improved engine performance and reduced exhaust emissions. Three independent variables (nozzle opening pressure, protrusion and engine speed) were used for the investigation of engine performance (brake power, BSFC and BTE) along with exhaust emissions (CO, HC, NOx and FSN).

NOP was changed from 230 bar (original) to 240 bar (modified) with 1.5 mm (original) washer at the injector seat to the 2.5 mm (modified) within a range of engine speed from 1000 to 2250 rpm. The engine was warmed up under control condition till it reached its working temperature. Then, the performance and emission parameters were tested at full throttle of fuel injection pump. The load was continuously added to bring the rpm down step by step. RSM technique was then applied on the experimental data in order to optimize engine performance. RSM not only predict responses but also mentions the most optimum conditions for the maximum efficient results. In order to check validation of RSM predicted values, the experiment than again performed only on optimum conditions.

2.2. Uncertainty analysis

Extent of accuracy of measure response variables and degree of error in each measurement of experimental setup can be determined through uncertainty analysis. Table 4 entails the measurable range of parameters, accuracy, and uncertainty in the ascertained values. However, the total uncertainty of experimental setup (U_{exp}) evaluated through following equation [51]:

$$U_{exp} = [\ (U_{HC})^2 + (U_{Speed})^2 + (U_{Power})^2 + (U_{FSN})^2 + (U_{CO})^2 + (U_{NOx})^2 + (U_{BSFC})^2\ ]^{1/2}$$

$$U_{exp} = [\ (1)^2 + (0.5)^2 + (1)^2 + (1)^2 + (1)^2 + (1)^2 + (0.5)^2\ ]^{1/2}$$

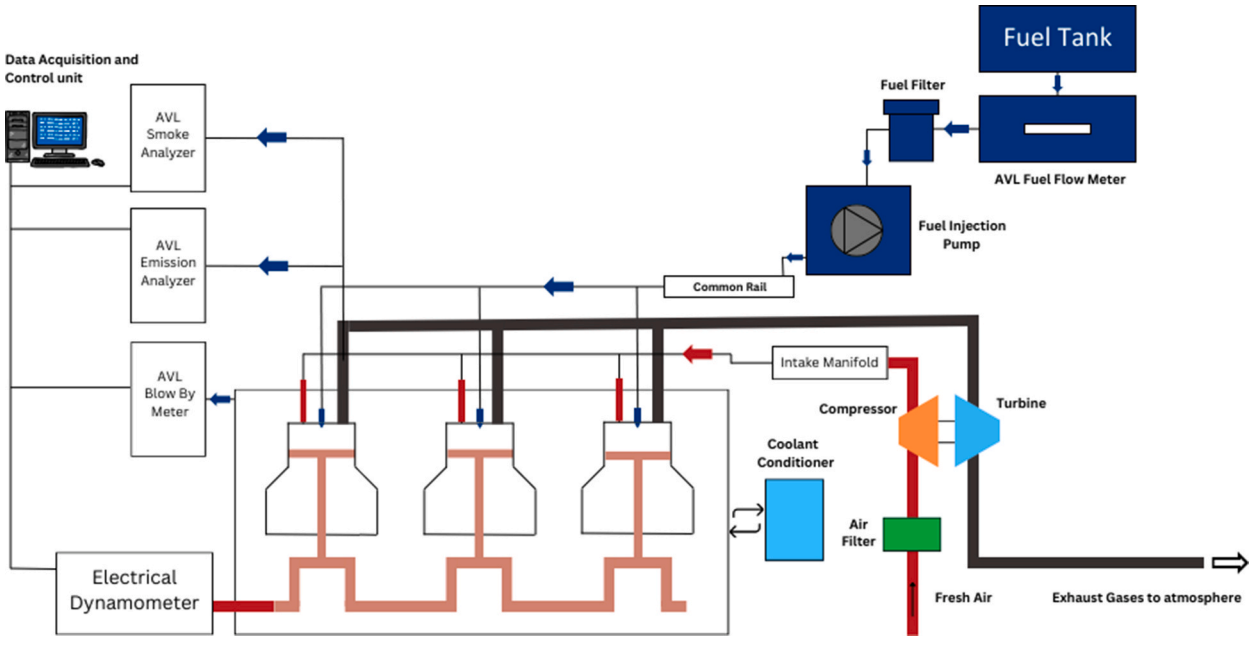

Fig. 1. Experimental setup.

Table 4
Measurable range, Accuracy and Uncertainty in measurements.

Parameters	Range measurable	Accuracy	Uncertainty (%)
HC	0–122.78 g/h	±2 g/h	±1 %
Speed	0–12000 rpm	±2 rpm	± 0.5
Power	0–500 kW	±0.5 kW	± 1
CO	0–828.88 g/h	±4 g/h	± 1
Fuel consumption	–	0.1 kg/kWh	± 0.5
NOx	0–1546.44 g/h	±6 g/h	± 1
FSN	0–10 %	±1 %	± 1

$$U_{exp} = 2.3\%$$

3. Results and discussion

3.1. Brake power (BP)

The trends of brake power with respect to engine speed and protrusion under 230 and 240 bar pressure can be seen in Fig. 2(a) and (b) respectively. It can be noticed that brake power generally increases with engine speed. The maximum brake power of 44.71 kW was obtained at 2250 rpm for 240 bar pressure and 1.5 mm protrusion. However, the minimum brake power of 17.53 kW was obtained at 1000 rpm for 240 bar pressure and 2.5 mm protrusion. At 230 bar pressure, when the protrusion increased from 1.5 to 2.5 mm, the brake power increased by 0.60 %. At 240 bar pressure, when the protrusion increased from 1.5 to 2.5 mm, the brake power decreased by 3.26 %. For protrusion 1.5 mm, when the pressure was increased from 230 to 240 bar, the brake power was increased by 1.82 %. For

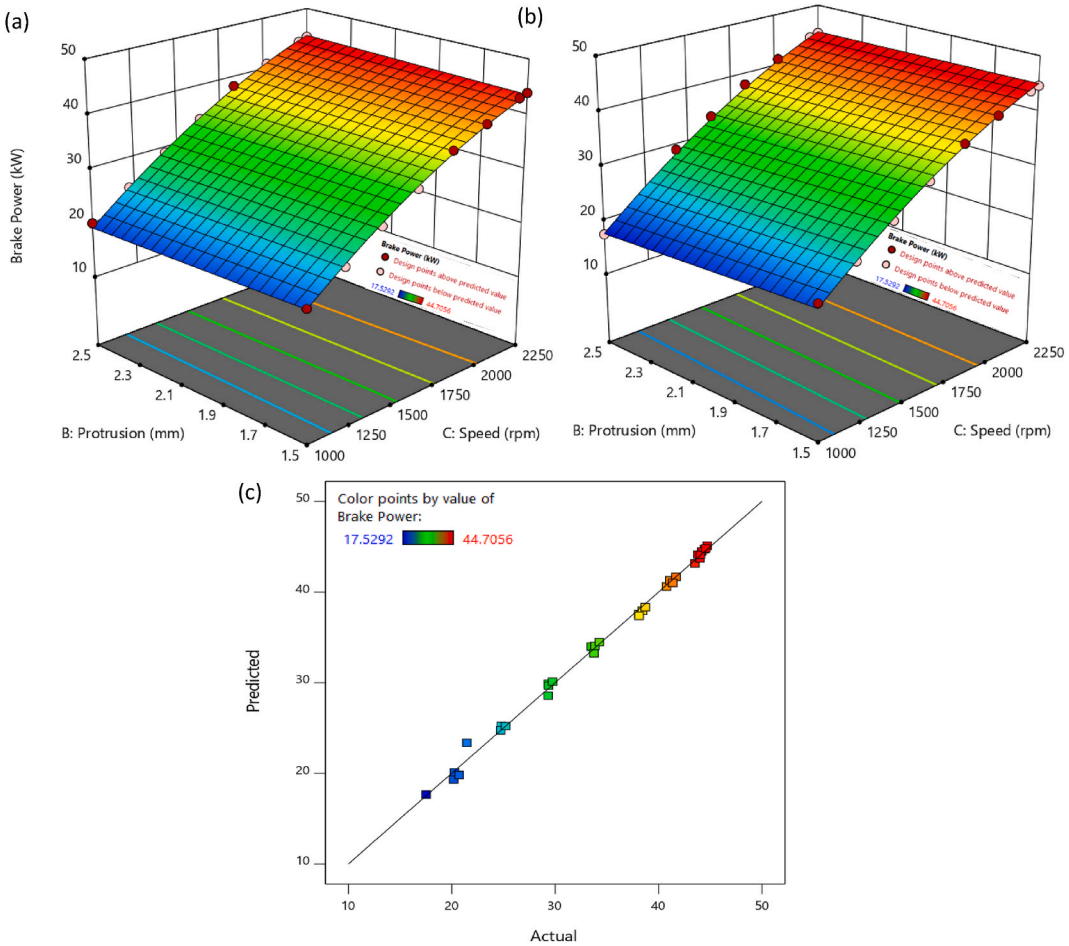

Fig. 2. BP comparison (a) at lower NOP, (b) at higher NOP, and (c) between empirical and predicted values.

protrusion 2.5 mm, when the pressure was increased from 230 to 240 bar, the brake power was decreased by 2.09 %. The engine usually misfires at higher injection pressure around 100 MPa due to excessive evaporation prior to ignition is not enough for adequate flame propagation [52]. The fuel droplets usually undergoes throttling process at higher injection pressure and these droplets end up approximately in vapor phase which ultimately results better combustion [53]. At higher fuel injection pressure and injection period, the more fuel spray impinge on cavity walls and mix with air along with reduction in nozzle area on extension of wall impingement [54].

Fig. 2 (c) shows the comparison between the experimental and predicted values of brake power. The blue color points represent the minimum brake power i.e., 17.53 kW whereas red color points show the maximum brake power i.e., 44.71 kW. ANOVA test is performed for brake power and the results are tabulated in Table 5. The F and p values are calculated which are 890.04 and smaller than 0.0001, respectively show that the measured brake power is statistically significant. In addition, the regression analysis shows that the data set is a good match with the regression line which shows that there is a very less difference between the predicted and actual values. Table 5 comprising of p-values indicate that the factors including fuel blends, engine load and speed are significant. The R^2 value (0.9962) was approximately equal to +1 and fair compliance between adjusted (0.9950) and predicted R^2 (0.9926) was observed with difference in their values equal to 0.01. The engine speed was radically contributed to accumulated variations with percentage contribution (PC%) of 99.0525 % in comparison with NOP and protrusion which were 0.0052 and 0.0982 % respectively. The poor fit in case of cubic and linear along with aliased nature of quadratic model are the main reasons for selection of best fitted quadratic model. Equation (1) depicts actual regression expression for brake power.

$$\text{Brake Power} = 34.45 - 0.0631A - 0.2748B + 12.68C - 0.3363AB + 0.4260AC + 0.4614BC - 2.54C^2 \quad (1)$$

Equation (1) shows the effect of independent variables on final response against each stipulated factor levels.

3.2. BSFC

The general trend of BSFC with the variation in engine speed and protrusion under 230 and 240 bar pressure can be observed from Fig. 3(a) and (b) respectively. It can be observed that BSFC was higher in the beginning, than BSFC started declining to a minimum value. However, after attaining the minimum value, the BSFC again started rising. This declining-rising behavior can be justified with more fuel consumption at the start for dominating inertial effect and to make engine in running condition. The lowest BSFC indicates optimum condition for engine operations and with the rise in engine speed, the more fuel started to consume for meeting higher power requirement [5]. At 230 bar pressure, when the protrusion increased from 1.5 to 2.5 mm, the BSFC increased by 2.16 %. At 240 bar pressure, when the protrusion increased from 1.5 to 2.5 mm, the BSFC decreased by 1.13 % as more uniform distribution in combustion result into lower BSFC [55]. For protrusion 1.5 mm, when the pressure was increased from 230 to 240 bar, the BSFC was decreased by 1.24 %. For protrusion 2.5 mm, when the pressure was increased from 230 to 240 bar, the BSFC was decreased by 4.43 %. The decline in BSFC can be reasoned to more effective fuel utilization at higher IP, as the improved fuel atomization linked with trivial delay in fuel injection owing to higher needle lift pressure with same time period and low amount of fuel enters into combustion chamber [56,57].

Fig. 3 (c) shows the comparison between the experimental and predicted values of BSFC. The blue color points represent the minimum BSFC i.e., 0.22kg/kWh whereas red color points show the maximum BSFC i.e., 0.28kg/kWh. ANOVA test is performed for BSFC and the results are tabulated in Table 6. The F and p values are calculated which are 30.91 and smaller than 0.0001, respectively show that the measured BSFC is statistically significant. In addition, the regression analysis shows that the data set is a good match with the regression line which shows that there is a very less difference between the predicted and actual values.

Table 6 comprising of p-values indicate that the factors including fuel blends, engine load and speed are significant. The R^2 value (0.9001) was approximately equal to +1 and fair compliance between adjusted (0.8710) and predicted R^2 (0.7830) was observed with difference in their values equal to 0.01. Both engine speed and NOP were radically influenced on accumulated variations with percentage contribution (PC%) of 76.1904 and 5.9523 % in contrast with protrusion (0.0035 %) respectively. The poor fit in case of cubic and linear along with aliased nature of quadratic model are the main reasons for selection of best fitted quadratic model. Equation (2) depicts actual regression expression for BSFC.

$$\text{BSFC} = 0.2372 - 0.0039A + 0.0003B - 0.0208C - 0.0020AB + 0.0042AC + 0.0036BC - 0.0102C^2 \quad (2)$$

Equation (2) shows the effect of independent variables on final response against each stipulated factor levels.

Table 5
ANOVA for reduced quadratic model (brake power).

Source	Sum of Squares	df	Mean Square	F-value	p-value	PC%
Model	2414.99	7	345.00	890.04	< 0.0001	99.6164
A-Nozzle Pressure	0.1254	1	0.1254	0.3235	0.5748	0.0052
B-Protrusion	2.38	1	2.38	6.13	0.0208	0.0982
C-Speed	2401.32	1	2401.32	6194.99	< 0.0001	99.0525
AB	3.62	1	3.62	9.34	0.0054	0.1493
AC	2.77	1	2.77	7.14	0.0133	0.1143
BC	3.25	1	3.25	8.38	0.0080	0.1341
C^2	30.45	1	30.45	78.55	< 0.0001	1.2560
Residual	9.30	24	0.3876			0.3836
Cor Total	2424.29	31				

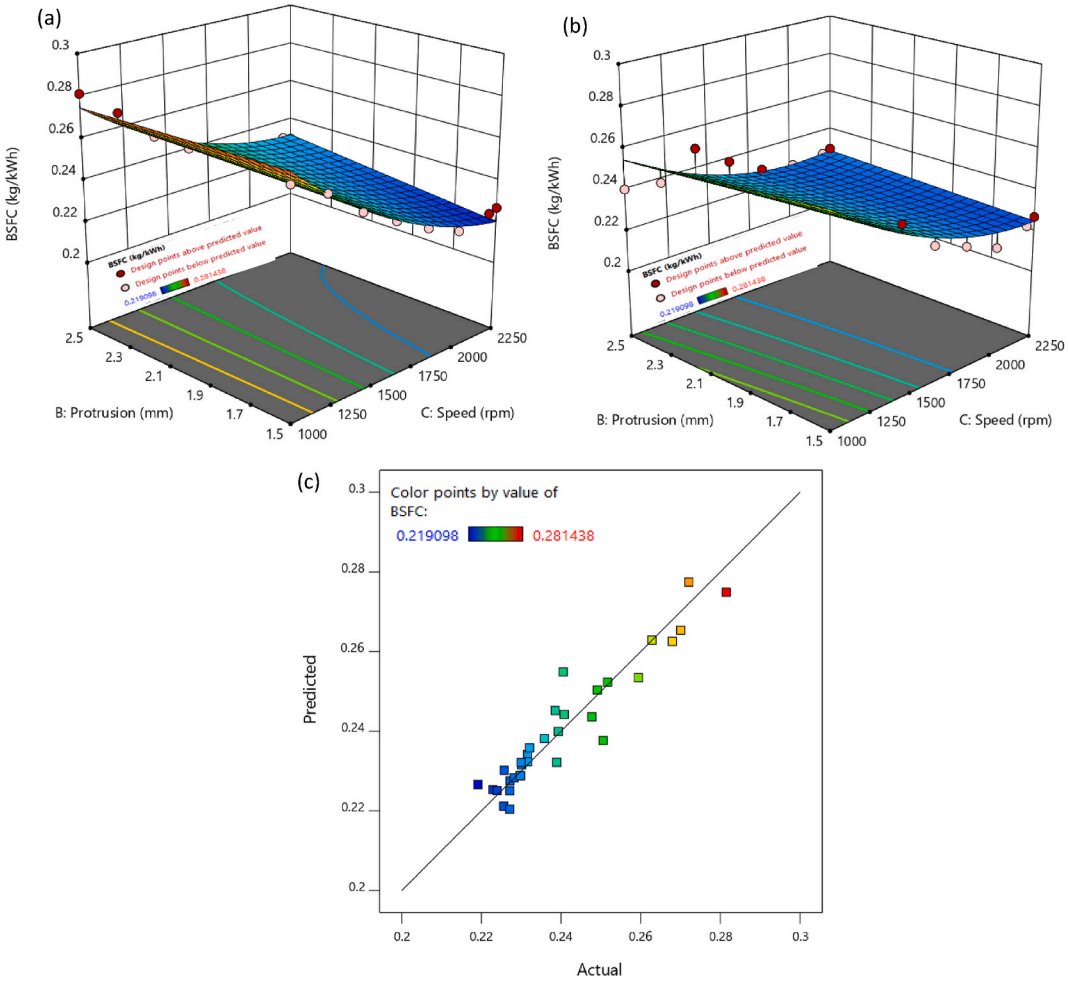

Fig. 3. BSFC comparison (a) under lower NOP, (b) under higher NOP, and (c) between empirical and predicted values.

Table 6
ANOVA for reduced quadratic model (BSFC).

Source	Sum of Squares	df	Mean Square	F-value	p-value	PC%
Model	0.0075	7	0.0011	30.91	< 0.0001	89.2857
A-Nozzle Pressure	0.0005	1	0.0005	13.40	0.0012	5.9523
B-Protrusion	2.963E-06	1	2.963E-06	0.0850	0.7732	3.53E-02
C-Speed	0.0064	1	0.0064	184.75	< 0.0001	76.1904
AB	0.0001	1	0.0001	3.60	0.0697	1.1904
AC	0.0003	1	0.0003	7.64	0.0108	3.5714
BC	0.0002	1	0.0002	5.59	0.0265	2.3809
C^2	0.0005	1	0.0005	14.05	0.0010	5.9523
Residual	0.0008	24	0.0000			9.5238
Cor Total	0.0084	31				

3.3. Brake thermal efficiency (BTE)

The increasing-decreasing BTE trend with respect to engine speed and protrusion under 230 and 240 bar pressure can be seen from Fig. 4 (a) and (b) respectively. BTE exhibits inverse relation with BSFC. Therefore, BTE was lower in the beginning, than it started to increase to a peak value. After attaining the peak, the BTE started to decline. This behavior can be reasoned with the amount of fuel consumption at lower and higher engine speeds. At 230 bar pressure, when the protrusion increased from 1.5 to 2.5 mm, the BTE decreased by 2.23 %. The fuel combustion quality is greatly affect by spray penetration length such that better combustion may produce by shorted spray lengths [58]. At 240 bar pressure, when the protrusion increased from 1.5 to 2.5 mm, the BTE incremented by 1.23 %. For protrusion 1.5 mm, when the pressure was incremented from 230 to 240 bar, the BTE was increased by 0.94 %. For

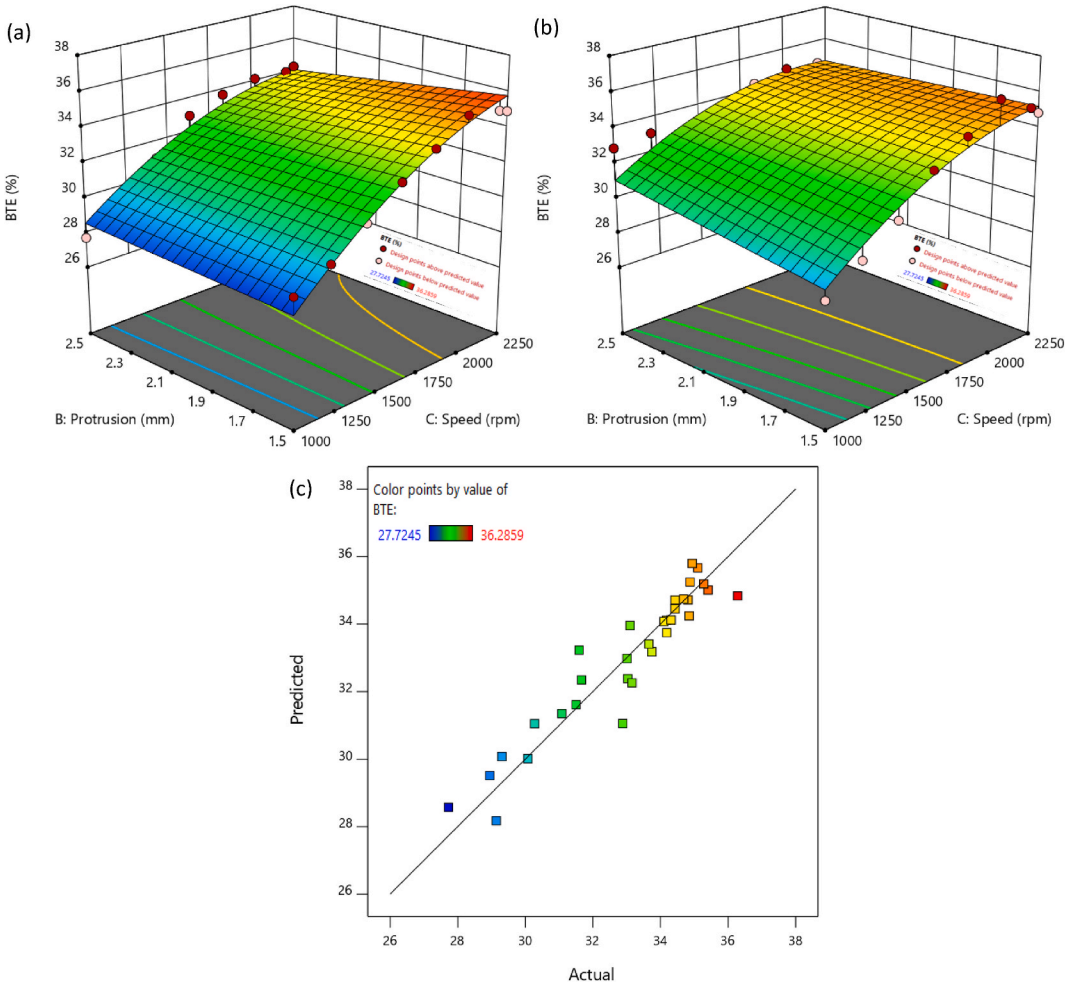

Fig. 4. BTE comparison (a) under lower NOP, (b) under higher NOP, and (c) between empirical and predicted values.

protrusion 2.5 mm, when the pressure was increased from 230 to 240 bar, the BTE was increased by 4.51 %. The higher nozzle pressures results increase in cylinder pressure and temperature which reduce combustion duration and heat release rate [59]. The increase in protrusion can prevent the spray from touching the bottom plane of cylinder head which may disrupt combustion process [60]. The quicker air flow may increase diesel penetration length by keeping it away from cylinder wall, resultantly BTE certainly improved for higher protrusion [30]. Fig. 4 (c) shows the comparison between the experimental and predicted values of BTE. The blue color points represent the minimum BTE i.e., 27.72 % whereas red color points show the maximum BTE i.e., 36.29 %. ANOVA test is performed for BTE and the results are tabulated in Table 5. The F and p values are calculated which are 28.73 and smaller than 0.0001, respectively show that the measured BTE is statistically significant. In addition, the regression analysis shows that the data set is a good match with the regression line which shows that there is a very less difference between the predicted and actual values.

Table 7
ANOVA in reduced quadratic model (BTE).

Source	Sum of Squares	df	Mean Square	F-value	p-value	PC%
Model	136.26	7	19.47	28.73	< 0.0001	89.3391
A-Nozzle Pressure	7.33	1	7.33	10.82	0.0031	4.8059
B-Protrusion	0.0368	1	0.0368	0.0542	0.8178	0.0241
C-Speed	118.82	1	118.82	175.36	< 0.0001	77.9045
AB	2.61	1	2.61	3.86	0.0613	1.7112
AC	3.42	1	3.42	5.04	0.0342	2.2423
BC	4.12	1	4.12	6.07	0.0213	2.7012
C^2	6.22	1	6.22	9.18	0.0058	4.0781
Residual	16.26	24	0.6776			10.6608
Cor Total	152.52	31				

Table 7 comprising of p-values indicate that the factors including fuel blends, engine load and speed are significant. The R^2 value (0.8934) was approximately equal to +1 and fair compliance between adjusted (0.8623) and predicted R^2 (0.7744) was observed with difference in their values equal to 0.01. Both engine speed and NOP were radically influenced on accumulated variations with percentage contribution (PC%) of 77.9045 and 4.8059 % in contrast to protrusion (0.0241 %) respectively. The poor fit in case of cubic and linear along with aliased nature of quadratic model are the main reasons for selection of best fitted quadratic model. Equation (3) depicts actual regression expression for BTE.

$$BTE = 33.30 + 0.4827A\text{-}0.0342B + 2.82C + 0.2857AB\text{-}0.4734AC\text{-}0.5194BC\text{-}1.15C^2 \quad (3)$$

Equation (3) shows the effect of independent variables on final response against each stipulated factor levels.

3.4. Filter smoke number (FSN)

FSN is an indicator of soot quantity presence in exhaust gasses. The variation in the trend of FSN with engine speed and protrusion for 230 and 240 bar pressure can be observed from Fig. 5 (a) and (b) respectively. It is noticeable that FSN is higher at lower speed, and it tends to be lower at higher engine speed. The higher FSN at lower engine speed is due to higher fuel consumption in order to tune engine in working condition by overcoming inertial effects. At 230 bar pressure, when the protrusion increased from 1.5 to 2.5 mm, the FSN decreased by 6.31 %. At 240 bar pressure, when the protrusion increased from 1.5 to 2.5 mm, the FSN decreased by 19.69 %. For protrusion 1.5 mm, when the pressure was increased from 230 to 240 bar, the FSN was increased by 0.68 %. For protrusion 2.5 mm, when the pressure was increased from 230 to 240 bar, the FSN was decreased by 13.07 %. The in cylinder temperature at lower pressure and protrusion is not suitable for oxidation which mainly responsible for formation of rich mixture and increased smoke emissions [61]. At higher pressure (240 bar) and longer protrusion (2.5 mm), the least indication of soot quality was found in comparison with other combination. It can be credited to better brake thermal efficiency under such condition. Moreover, the higher injection pressure consequently shortens the ignition delay especially for larger fuel mass. The higher pressure also reduces the flame

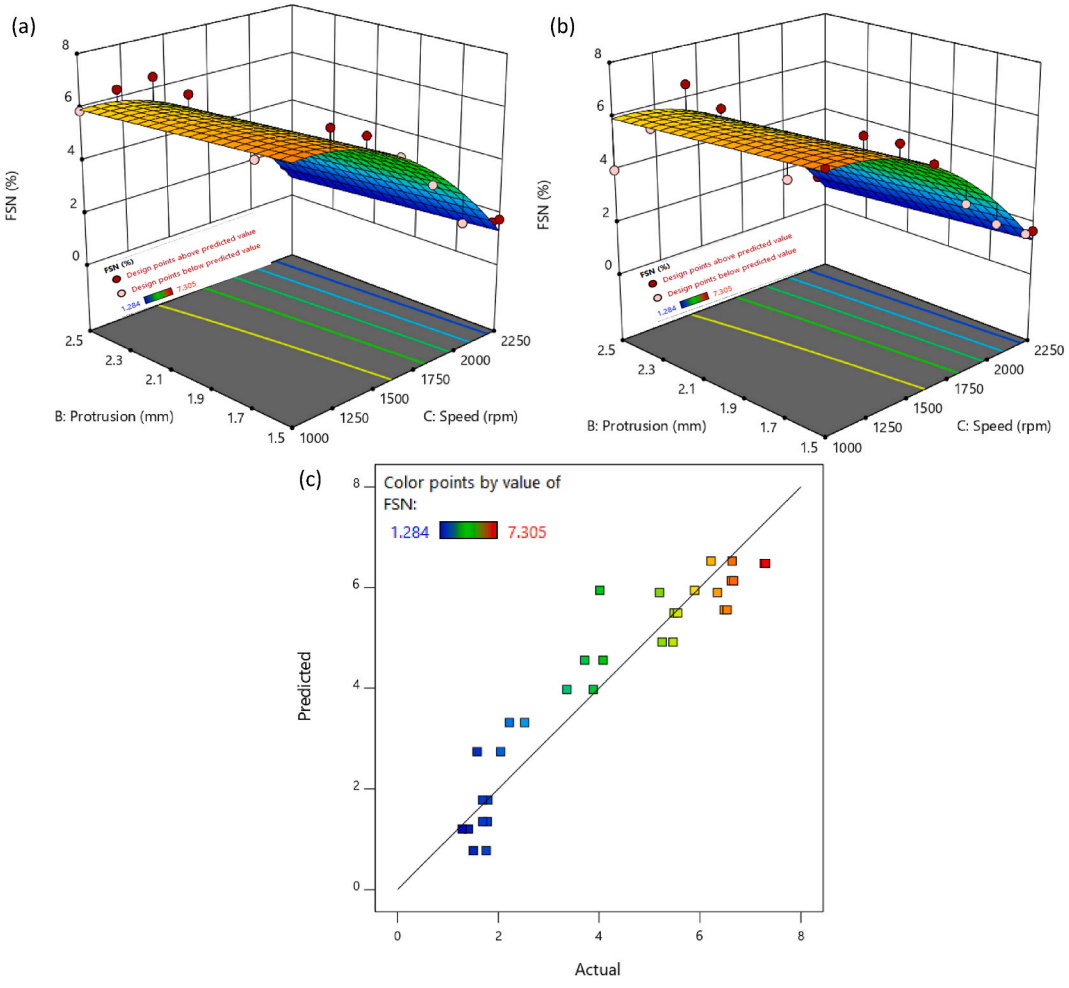

Fig. 5. FSN comparison (a) under lower NOP, (b) under higher NOP, and (c) between empirical and predicted values.

area and consequently more unburned fuel left owing to higher evaporation and heat absorption [52]. As per the previous literature [62,63], the oxidation rate becomes sufficient to improve air-fuel droplets mixing and resultantly produce higher cylinder temperature. The prolonged ignition period and higher combustion temperature mainly responsible for attenuation of smoke and soot emissions.

Fig. 5 (c) shows the comparison between the experimental and predicted values of FSN. The blue color points represent the minimum FSN i.e., 1.28 % whereas red color points show the maximum FSN i.e., 7.31 %. ANOVA test is performed for FSN and the results are tabulated in Table 8. The F and p values are calculated which are 74.90 and smaller than 0.0001, respectively show that the measured FSN is statistically significant. In addition, the regression analysis shows that the data set is a good match with the regression line which shows that there is a very less difference between the predicted and empirical values.

Table 8 comprising of p-values indicate that the factors including fuel blends, engine load and speed are significant. The R^2 value (0.8892) was approximately equal to +1 and fair compliance between adjusted (0.8773) and predicted R^2 (0.8509) was observed with difference in their values equal to 0.01. The poor fit in case of cubic and linear along with aliased nature of quadratic model are the main reasons for selection of best fitted quadratic model. Equation (4) depicts actual regression expression for FSN.

$$FSN = 5.10–0.2890B\text{-}2.59C–1.45C^2 \quad (4)$$

Equation (4) shows the effect of independent variables on final response against each stipulated factor levels.

3.5. CO emission

Fig. 6(a) and (b) demonstrates the change in CO emission with respect to fuel injection pressure, engine speed and nozzle penetration length (protrusion). It can be clearly seen from figures that fuel injection pressure is the most significant factor in declining the CO emission. At 230 bar pressure, when the protrusion increased from 1.5 to 2.5 mm, the CO emission increased by 3.82 %. At 240 bar pressure, when the protrusion increased from 1.5 to 2.5 mm, the CO emission decreased by 3.61 %. For protrusion 1.5 mm, when the pressure was increased from 230 to 240 bar, the CO emission was decreased by 4.47 %. For protrusion 2.5 mm, when the pressure was increased from 230 to 240 bar, the CO emission was decreased by 11.31 %. The higher fuel injection pressure finely atomizes fuel molecules and increases spray penetration which ultimately results better combustion [47]. The results obtained in the current study also coincides with previous research [41].

Fig. 6 (c) represents the comparative view among emprical and predicted values of CO emission. A blue color points represent the minimum CO contents i.e., 80 g/h whereas red color points show the maximum CO contents i.e., 215 g/h. ANOVA test is performed for CO emissions and the results are tabulated in Table 9. The F and p values are calculated which are 200.61 and smaller than 0.0001, respectively show that the measured CO contents are statistically significant. In addition, the regression analysis shows that the data set is a good match with the regression line which shows that there is a very less difference between the predicted and empirical values.

Table 9 comprising of p-values indicate that the factors including fuel blends, engine load and speed are significant. The R^2 value (0.9747) was approximately equal to +1 and fair compliance between adjusted (0.9699) and predicted R^2 (0.9603) was observed with difference in their values equal to 0.01. Both engine speed and NOP were radically influenced on accumulated variations with percentage contribution (PC%) of 78.5165 and 1.7480 % in contrast to protrusion (0.0009 %) respectively. The poor fit in case of cubic and linear along with aliased nature of quadratic model are the main reasons for selection of best fitted quadratic model. Equation (5) depicts actual regression expression for CO emission.

$$CO = 111.92–5.44A + 0.1250B + 53.33C\text{-}2.44AB+29.96C^2 \quad (5)$$

Equation (5) shows the effect of independent variables on final response against each stipulated factor levels.

3.6. HC emission

Hydrocarbon (HC) emissions are the result of inappropriate mixing of air and fuel molecules or large sized fuel droplets [64]. It is evident that HC emission decreases with the increase in pressure. It can be credited to good mixing between air and fuel mixture mainly due to fine spray at higher pressure [47]. The hydrocarbon emission was higher initially but the trend was declined at higher rpm. The general declining trend of HC emission along with engine speed (rpm) due to higher combustion temperature, lower flame quenching to cylinder walls and adsorption or desorption in oil film [5]. Fig. 7(a) and (b) depicts the variation in HC emission with respect to protrusion for 230 and 240 bar pressure respectively along with engine speed. At 230 bar pressure, when the protrusion increased from 1.5 to 2.5 mm, the HC emission increased by 2.86 %. At 240 bar pressure, when the protrusion increased from 1.5 to 2.5 mm, the HC emission decreased by 4.23 %. For protrusion 1.5 mm, when the pressure was increased from 230 to 240 bar, the HC emission was

Table 8
ANOVA in reduced quadratic model (FSN).

Source	Sum of Squares	df	Mean Square	F-value	p-value	PC%
Model	124.10	3	41.37	74.90	< 0.0001	8.01E+01
B-Protrusion	2.67	1	2.67	4.84	0.0363	1.26E+00
C-Speed	99.93	1	99.93	180.93	< 0.0001	2.71E-03
C^2	9.97	1	9.97	18.06	0.0002	7.88E+01
Residual	15.47	28	0.5523			1.99E+01
Cor Total	139.57	31				

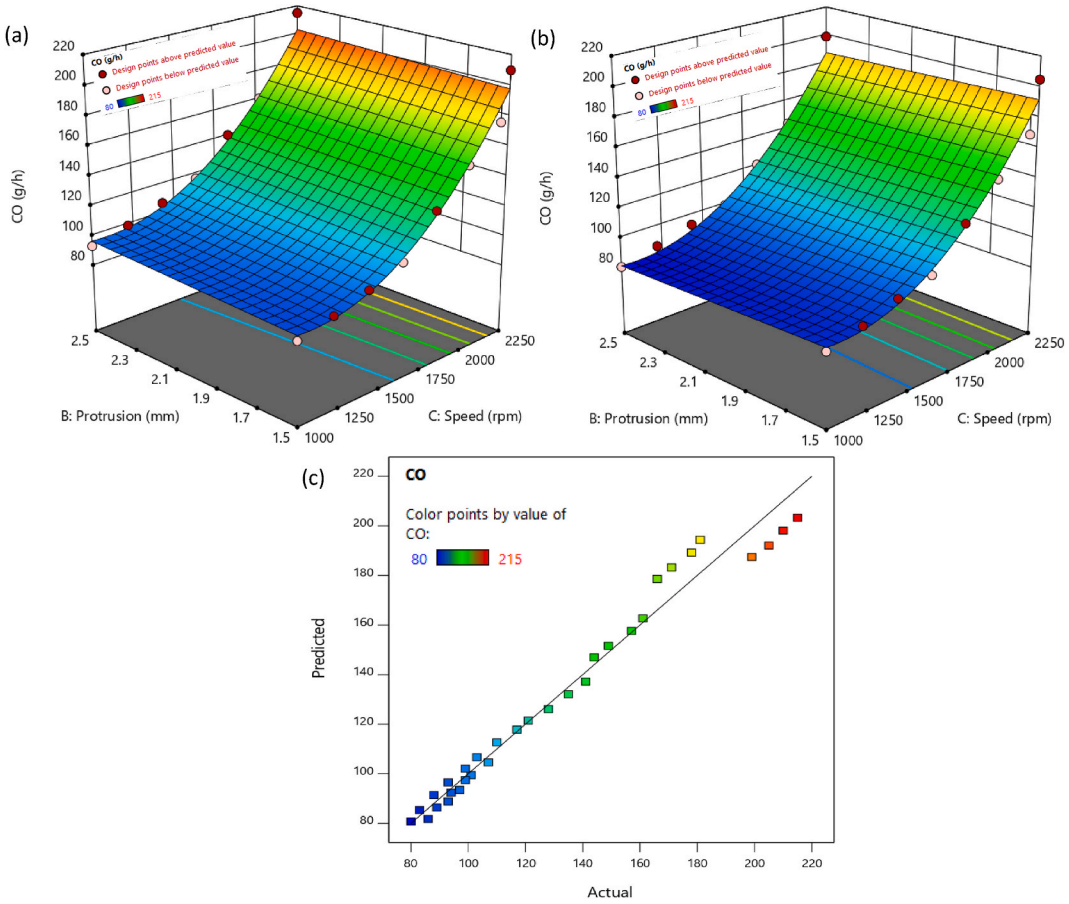

Fig. 6. CO content comparison (a) under lower NOP, (b) under higher NOP, and (c) between empirical and predicted values.

Table 9
ANOVA in reduced quadratic model (CO emission).

Source	Sum of Squares	df	Mean Square	F-value	p-value	PC%
Model	52756.48	5	10551.30	200.61	< 0.0001	97.4733
A-Nozzle Pressure	946.13	1	946.13	17.99	0.0002	1.7480
B-Protrusion	0.5000	1	0.5000	0.0095	0.9231	0.0009
C-Speed	42496.29	1	42496.29	807.96	< 0.0001	78.5165
AB	190.13	1	190.13	3.61	0.0684	0.3512
C^2	4229.59	1	4229.59	80.41	< 0.0001	7.8146
Residual	1367.52	26	52.60			2.5266
Cor Total	54124.00	31				

decreased by 1.86 %. For protrusion 2.5 mm, when the pressure was increased from 230 to 240 bar, the HC emission was decreased by 8.62 %.

Fig. 7 (c) shows the comparison between the experimental and predicted values of HC emission. The blue color points represent the minimum HC contents i.e., 0.73 g/h whereas red color points show the maximum CO contents i.e., 1.1 g/h. ANOVA test is performed for HC emissions and the results are tabulated in Table 10. The F and p values are calculated which are 178.43 and smaller than 0.0001, respectively show that the measured HC contents are statistically significant. In addition, the regression analysis shows that the data set is a good match with the regression line which shows that there is a very less difference between the predicted and empirical values.

Table 10 comprising of p-values indicate that the factors including fuel blends, engine load and speed are significant. The R^2 value (0.9772) was approximately equal to +1 and fair compliance between adjusted (0.9717) and predicted R^2 (0.9547) was observed with difference in their values equal to 0.01. Both engine speed and NOP were radically influenced on accumulated variations with percentage contribution (PC%) of 86.8174 and 7.2932 % in contrast to protrusion (0.1170 %) respectively. The poor fit in case of cubic and linear along with aliased nature of quadratic model are the main reasons for selection of best fitted quadratic model. Equation (6) depicts actual regression expression for HC emission.

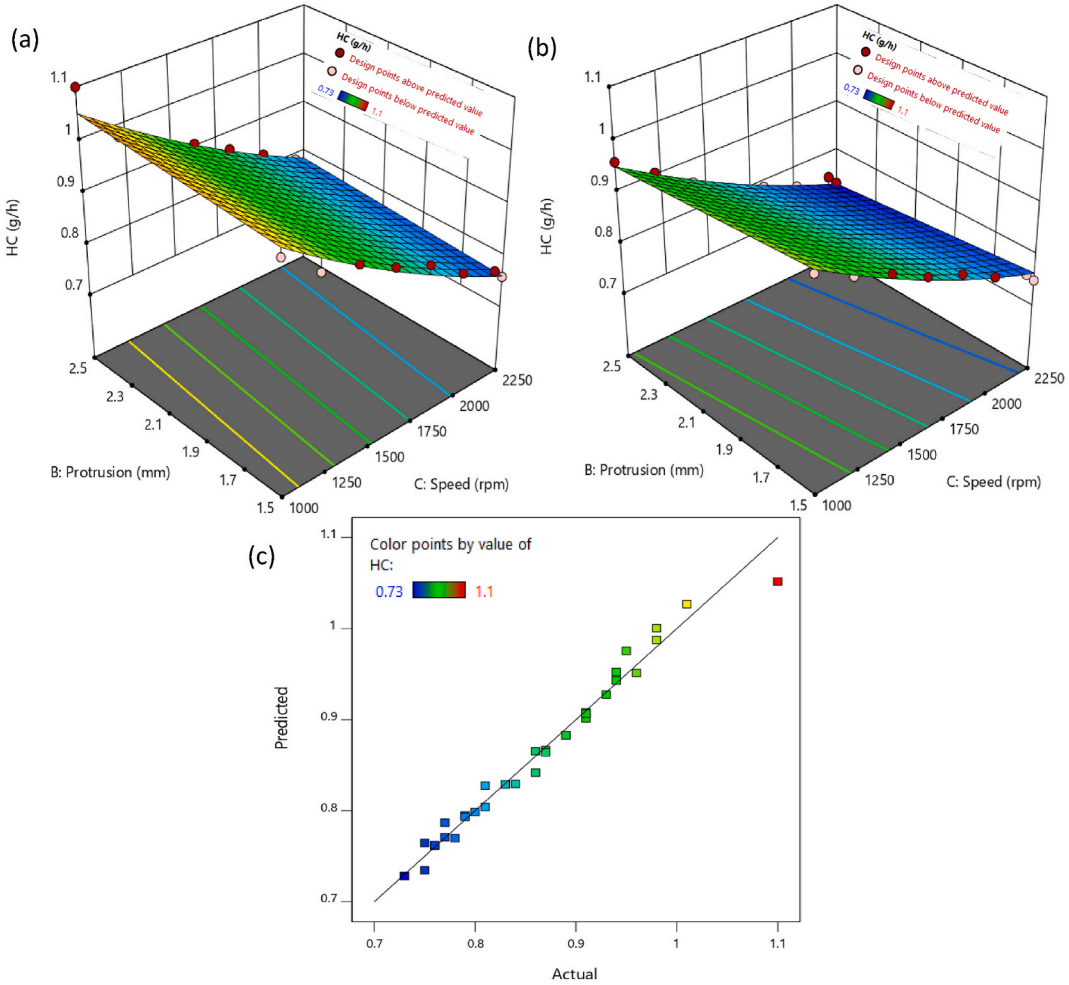

Fig. 7. HC comparison (a) under lower NOP, (b) under higher NOP and (c) between empirical and predicted values.

Table 10
ANOVA in reduced quadratic model (HC emission).

Source	Sum of Squares	df	Mean Square	F-value	p-value	PC%
Model	0.2506	6	0.0418	178.43	< 0.0001	97.7379
A-Nozzle Pressure	0.0187	1	0.0187	79.94	< 0.0001	7.2932
B-Protrusion	0.0003	1	0.0003	1.08	0.3083	0.1170
C-Speed	0.2226	1	0.2226	950.85	< 0.0001	86.8174
AB	0.0075	1	0.0075	32.05	< 0.0001	2.9251
AC	0.0017	1	0.0017	7.23	0.0126	0.6630
C^2	0.0013	1	0.0013	5.60	0.0260	0.5070
Residual	0.0059	25	0.0002			2.3010
Cor Total	0.2564	31				

$$HC = 0.8657–0.0244A-0.0028B-0.1220C-0.0153AB+0.0105AC+0.01677C^2 \quad (6)$$

Equation (6) shows the effect of independent variables on final response against each stipulated factor levels.

3.7. NOx emission

Fig. 8 (a) and (b) designates the formation of NOx contents against variation in engine speed and protrusion under 230 and 240 bar pressure respectively. NOx emissions are the prime function of cylinder temperature. As the combustion temperature increases, NOx will also increase. It has been studied that the for increase in fuel injection temperature, the fuel atomization gets better which result in higher heat release rate and combustion temperature [47]. The highest NOx of 410 g/h was obtained at 2250 rpm, 2.5 mm protrusion

and 240 bar pressure. At 230 bar pressure, when the protrusion increased from 1.5 to 2.5 mm, the NOx emission decreased by 2.5 %. At 240 bar pressure, when the protrusion increased from 1.5 to 2.5 mm, the NOx emission increased by 2.89 %. For protrusion 1.5 mm, when the pressure was increased from 230 to 240 bar, the NOx emission was increased by 2.18 %. For protrusion 2.5 mm, when the pressure was increased from 230 to 240 bar, the NOx emission was increased by 7.83 %. The combination of higher nozzle pressure and protrusion significantly increased the NOx emission due to better fuel atomization and air-fuel mixture [65,66].

Fig. 8 (c) shows the comparison between the experimental and predicted values of NOx emission. The blue color points represent the minimum NOx contents i.e., 209 g/h whereas red color points show the maximum NOx contents i.e., 410 g/h. ANOVA test is performed for NOx emissions and the results are tabulated in Table 11. The F and p values are calculated which are 37.55 and smaller than 0.0001, respectively show that the measured NOx contents are statistically significant. In addition, the regression analysis shows that the data set is a good match with the regression line which shows that there is a very less difference between the predicted and empirical values.

Table 11 comprising of p-values indicate that the factors including fuel blends, engine load and speed are significant. The R^2 value (0.8009) was approximately equal to +1 and fair compliance between adjusted (0.7796) and predicted R^2 (0.7359) was observed with difference in their values equal to 0.01. The poor fit in case of cubic and linear along with aliased nature of quadratic model are the main reasons for selection of best fitted quadratic model. Equation (7) depicts actual regression expression for NOx emission.

$$NOx = 271.37 + 6.75A + 0.3125B + 77.19C \quad (7)$$

Equation (7) shows the effect of independent variables on final response against each stipulated factor levels.

3.8. RSM based optimization

RSM is multi objective optimization technique in which multiple factors are optimized to achieve target output by developing relation between input and response variables [67]. Design Expert software was employed to implement RSM on the empirical data including engine performance and emission. An optimization setup demarcated in Table 12, is intended at maximizing brake power and BTE. However, BSFC, CO, HC, FSN and NO_x were targeted to their minimization. All response variables have been assigned with the default weight of 3 in order to carry equal importance. Fig. 9 depicts that the engine operating conditions as optimized by RSM model were 240 bar pressure, 2.5 mm protrusion and 1935.67 engine rpm. The response variables were achieved as 39.89 kW W brake power, 0.23kg/kwh BSFC, 34.66 % BTE, 138.09 g/h CO emission, 0.77 g/h HC emission, 316.79 g/h NOx emission and 3.17 % FSN with respect to optimal conditions.

The composite desirability (D) analyses the statistical reliability of response variables of optimization setup. D value ranges from zero to one with no unit, as one represents most effective optimization. D value was achieved as 0.712 for the designated targets, and this is an obvious sign of favourable outcomes from optimization settings for all input and response variables. Fig. 10 represents both composite (D) and individual desirability (d) for deep analysis and understanding of the effect of each response variables.

The highest and least d value were obtained for HC (0.89) and NOx (0.46) respectively. The numeric values indicates that any change in HC emission would be responsible for the greatest variations in the model while any change in NOx would create minimum variations on overall model. Table 13 displays the comparison between RSM predicted values and experimentally validated values. The experimentation was then performed as per RSM optimized input factors (Nozzle pressure (240 bar), Protrusion (2.5 mm) and Engine speed (1936 rpm)). The highest absolute percentage error (APE) of 4.42 % was obtained for NOx emission and lowest APE of 2.89 % was obtained for BSFC.

4. Conclusions

The following conclusions were obtained on performing the experiment under different fuel injection conditions.

- The brake power was increased by 1.82 % for 1.5 mm nozzle protrusion, when the pressure was increased from 230 to 240 bar. At 240 bar pressure, when the protrusion increased from 1.5 to 2.5 mm, the BTE increased by 1.23 %.
- FSN decreased by 19.69 % at 240 bar pressure, when the protrusion increased from 1.5 to 2.5 mm. CO emission was decreased by 4.47 and 11.31 % for protrusion 1.5–2.5 mm, when the pressure was increased from 230 to 240 bar, respectively.
- When the nozzle protrusion changed from 1.5 mm to 2.5 mm, the NOx emission was increased by 2.18 % and 7.83 %. However, at 230 bar pressure, when the protrusion increased from 1.5 to 2.5 mm, the HC emission increased by 2.86 %. Whereas for 240 bar pressure, the HC emission decreased by 4.23 %.
- The nozzle protrusion predominantly affected brake power as compared to nozzle opening pressure. The brake power decreased with the increase in protrusion. The nozzle opening pressure (NOP) predominantly affected the fuel conversion efficiency of engine as compared to protrusion. The higher NOP leads to better fuel atomization and air fuel mixing which ultimately reflects homogeneous air-fuel mixing and improved fuel conversion efficiency. FSN, CO and NOx possess inverse relation with nozzle opening pressure and protrusion due to better fuel atomization at higher NOP and protrusion.
- The engine operating conditions as optimized by RSM model were 240 bar pressure, 2.5 mm protrusion and 1935.67 engine rpm. The response variables were achieved as 39.89 kW W brake power, 0.23kg/kwh BSFC, 34.66 % BTE, 138.09 g/h CO emission, 0.77 g/h HC emission, 316.79 g/h NOx emission and 3.17 % FSN with respect to these optimal conditions. The experiment was again performed on the RSM optimized input factors. The highest absolute percentage error (APE) of 4.42 % was obtained for NOx emission and lowest APE of 2.89 % was obtained for BSFC.

In future, combining RSM with CFD simulations will allow a more comprehensive optimization approach. The future of engine

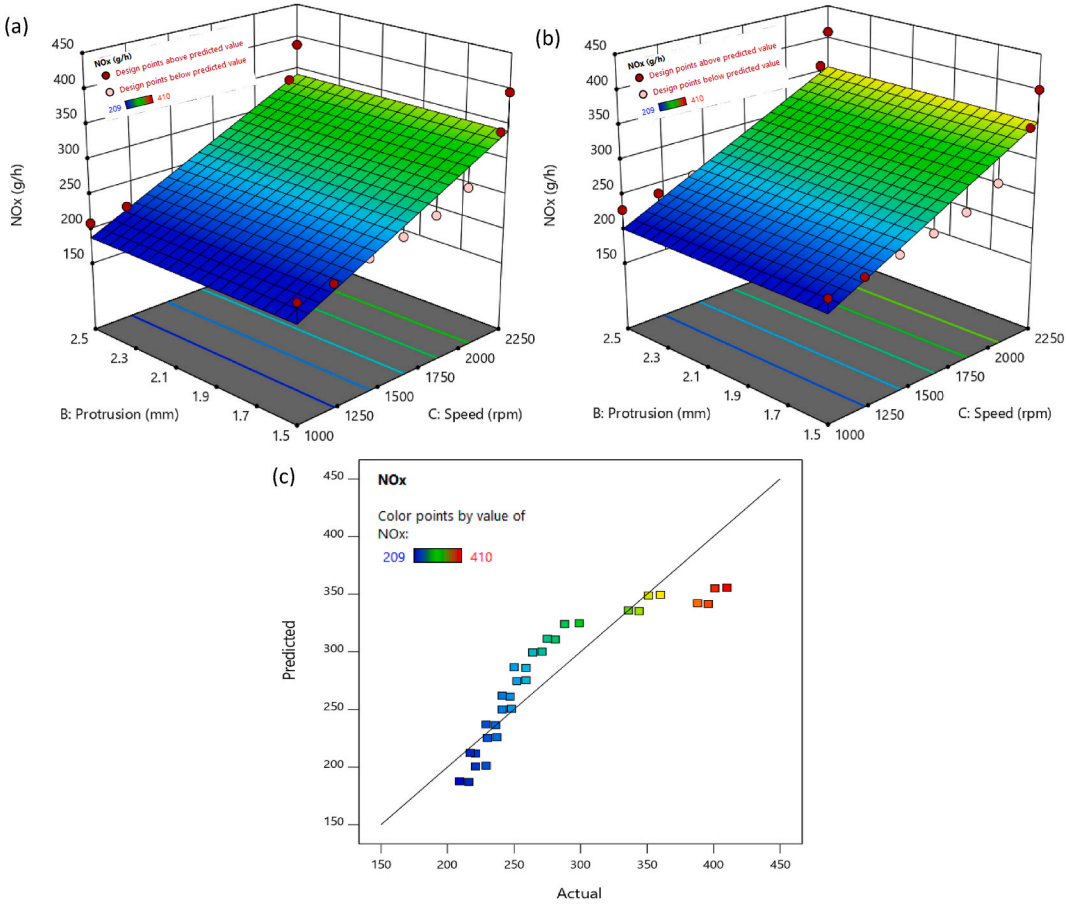

Fig. 8. NOx comparison (a) under lower NOP, (b) under higher NOP, and (c) between empirical and predicted values.

Table 11
ANOVA in reduced quadratic model (NOx emission).

Source	Sum of Squares	df	Mean Square	F-value	p-value	PC%
Model	92353.34	3	30784.45	37.55	< 0.0001	0.80
A-Nozzle Pressure	1458.00	1	1458.00	1.78	0.1931	0.012
B-Protrusion	3.13	1	3.13	0.0038	0.9512	2.72 E−05
C-Speed	90892.22	1	90892.22	110.88	< 0.0001	0.7883
Residual	22953.53	28	819.77			0.1990
Cor Total	1.153E+05	31				

Table 12
Optimization setup.

Name	Goal	Lower Limit	Upper Limit	Lower Weight	Upper Weight	Importance
A: Nozzle Pressure	In range	230	240	1	1	3
B: Protrusion	In range	1.5	2.5	1	1	3
C: Speed	In range	1000	2250	1	1	3
Brake Power	maximize	17.5292	44.7056	1	1	3
BSFC	minimize	0.219098	0.281438	1	1	3
BTE	maximize	27.7245	36.2859	1	1	3
CO	minimize	80	215	1	1	3
HC	minimize	0.73	1.1	1	1	3
NOx	minimize	209	410	1	1	3
FSN	minimize	1.284	7.305	1	1	3

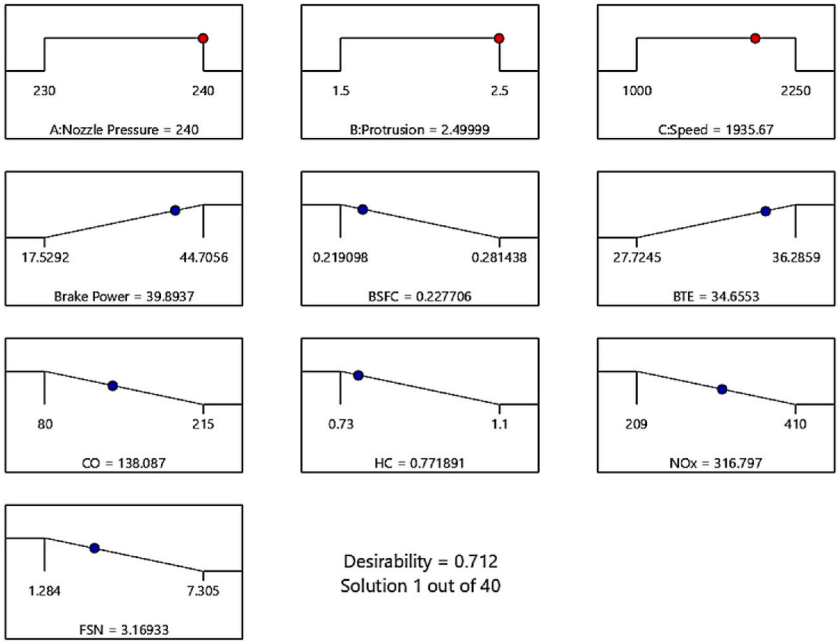

Fig. 9. Ramp charts for desirability function for each input and response parameters.

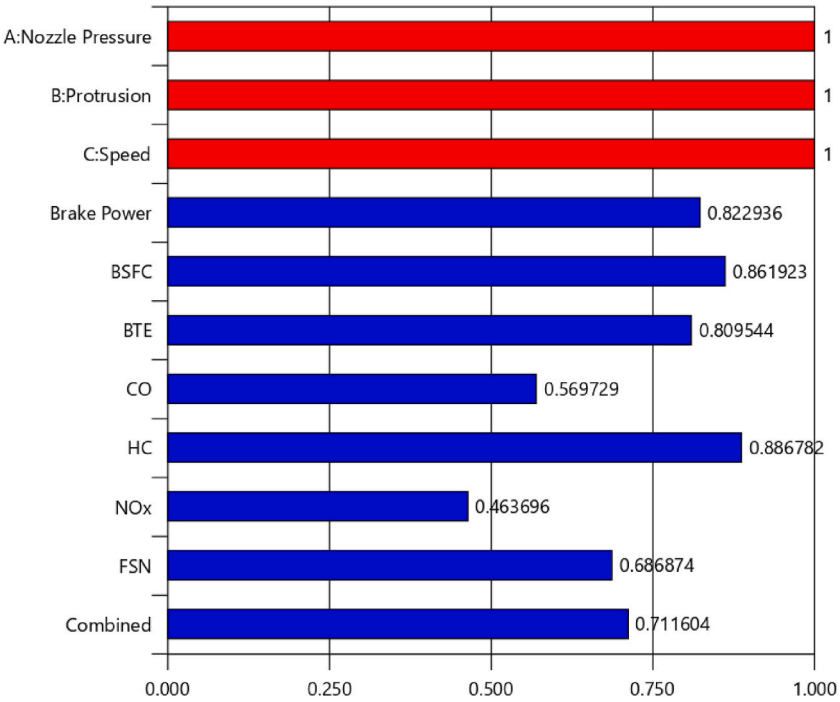

Fig. 10. Desirability chart for optimization setup.

design will heavily rely on numerical simulations, and RSM can be used to create surrogate models that interact with CFD to optimize parameters like combustion chamber geometry, injector design, and valve timing. Future engines may require real-time optimization and adaptive control to respond to changing operating conditions and environmental regulations. RSM-based algorithms can continuously adapt engine parameters to maximize performance and minimize emissions while maintaining compliance with regulations.

Table 13
Comparative analysis among optimized and empirical values.

Responses	Input factors (Nozzle pressure (240 bar), Protrusion (2.5 mm) and Engine speed (1936 rpm))		
	RSM Predicted	Empirical	APE
BP (kW)	39.8937	38.6131	3.21
HC (g/h)	0.7719	0.7532	2.41
BSFC (kg/kWh)	0.2277	0.2211	2.89
NOx (g/h)	316.797	302.7946	4.42
BTE (%)	34.6553	33.4215	3.56
CO (g/h)	138.087	132.2045	4.26
FSN (%)	3.1693	3.0422	4.01

Author statement

Conceptualization, Muhammad Usman.
Methodology, Muhammad Usman, Muhammad Kashif Tariq.
Formal analysis, Fahid Riaz.
Software, Muhammad Ali Ijaz Malik, Fahid Riaz.
Resources, Yasser Fouad, Fahid Riaz.
Investigation, Muhammad Usman, Muhammad Imran Masood.
Validation, Muhammad Kashif Tariq, Bashar Shboul.
Supervision, Muhammad Usman, Muhammad Imran Masood.
Writing - Original Draft, Muhammad Ali Ijaz Malik, Muhammad Kashif Tariq.
Funding acquisition, Yasser Fouad.
Writing - Review & Editing, Yasser Fouad, Bashar Shboul.

Declaration of competing interest

The authors declare that they have no known competing financial interests or personal relationships that could have appeared to influence the work reported in this paper.

Data availability

No data was used for the research described in the article.

Acknowledgements

The authors extend their appreciation to Deputyship for research and innovation, “Ministry of Education” in Saudi Arabia for funding this research (IFKSUOR3-273-4).

References

[1] G. Kalghatgi, Is it really the end of internal combustion engines and petroleum in transport? Appl. Energy 225 (2018) 965–974.
[2] M.U. Hassan, et al., Tribological analysis of molybdenum disulfide (MOS2) additivated in the Castor and mineral oil used in diesel engine, Sustainability 14 (17) (2022), 10485.
[3] Z.U. Hassan, et al., Use of diesel and emulsified diesel in CI engine: a comparative analysis of engine characteristics, Sci. Prog. 104 (2) (2021), 00368504211020930.
[4] M. Usman, et al., Comparative assessment of ethanol and methanol–ethanol blends with gasoline in SI engine for sustainable development, Sustainability 15 (9) (2023) 7601.
[5] M.A. Ijaz Malik, et al., Experimental evaluation of methanol-gasoline fuel blend on performance, emissions and lubricant oil deterioration in SI engine, Adv. Mech. Eng. 13 (6) (2021), 16878140211025213.
[6] M.A.I. Malik, et al., Use of methanol-gasoline blend: a comparison of SI engine characteristics and lubricant oil condition, J. Chin. Inst. Eng. 45 (5) (2022) 402–412.
[7] A. Jain, A.P. Singh, A.K. Agarwal, Effect of fuel injection parameters on combustion stability and emissions of a mineral diesel fueled partially premixed charge compression ignition (PCCI) engine, Appl. Energy 190 (2017) 658–669.
[8] A.A. Babadi, et al., Emerging technologies for biodiesel production: processes, challenges, and opportunities, Biomass Bioenergy 163 (2022), 106521.
[9] M. Usman, et al., Experimental assessment of performance, emission and lube oil deterioration using gasoline and LPG for a sustainable environment, Case Stud. Therm. Eng. 49 (2023), 103300.
[10] B. Dhinesh, et al., A numerical and experimental assessment of a coated diesel engine powered by high-performance nano biofuel, Energy Convers. Manag. 171 (2018) 815–824.
[11] G. Sujesh, S. Ramesh, Modeling and control of diesel engines: a systematic review, Alex. Eng. J. 57 (4) (2018) 4033–4048.
[12] A.S. Ayodhya, K.G. Narayanappa, An overview of after-treatment systems for diesel engines, Environ. Sci. Pollut. Control Ser. 25 (35) (2018) 35034–35047.
[13] A. Ahmed, et al., Environment-friendly novel fuel additives: investigation of the effects of graphite nanoparticles on performance and regulated gaseous emissions of CI engine, Energy Convers. Manag. 211 (2020), 112748.
[14] M. Usman, et al., Response surface methodology routed optimization of performance of hydroxy gas enriched diesel fuel in compression ignition engines, Processes 9 (8) (2021) 1355.
[15] M. Usman, et al., Acetone–Gasoline blend as an alternative fuel in SI engines: a novel comparison of performance, emission, and lube oil degradation, ACS Omega 8 (12) (2023) 11267–11280.
[16] A. Celik, M. Yilmaz, O.F. Yildiz, Improvement of diesel engine startability under low temperatures by vortex tubes, Energy Rep. 6 (2020) 17–27.

[17] B. Mohan, W. Yang, S. kiang Chou, Fuel injection strategies for performance improvement and emissions reduction in compression ignition engines—a review, Renew. Sustain. Energy Rev. 28 (2013) 664–676.
[18] A.T. Doppalapudi, A. Azad, M. Khan, Combustion chamber modifications to improve diesel engine performance and reduce emissions: a review, Renew. Sustain. Energy Rev. 152 (2021), 111683.
[19] J. Thangaraja, C. Kannan, Effect of exhaust gas recirculation on advanced diesel combustion and alternate fuels-A review, Appl. Energy 180 (2016) 169–184.
[20] S. Gopinath, et al., Effect of spray characteristics influences combustion in DI diesel engine–A review, Mater. Today: Proc. 33 (2020) 52–65.
[21] M. Arai, Physics behind diesel sprays, in: Proc. Of ICLASS, 12th Triennial International Conference on Liquid Atomization and Spray Systems, Sept. 2012. Heidelberg, Germany.
[22] P. Aleiferis, N. Papadopoulos, Heat and mass transfer effects in the nozzle of a fuel injector from the start of needle lift to after the end of injection in the presence of fuel dribble and air entrainment, Int. J. Heat Mass Tran. 165 (2021), 120576.
[23] N. Khayum, A. Subramanian, M. Sivalingam, Effect of nozzle opening pressure on combustion, performance, and emission analyses of a dual fuel diesel engine, Energy Sources, Part A Recovery, Util. Environ. Eff. (2020) 1–20.
[24] Z. Li, et al., Parametric study of a single-channel diesel/methanol dual-fuel injector on a diesel engine fueled with directly injected methanol and pilot diesel, Fuel 302 (2021), 121156.
[25] K. Akkoli, et al., Effect of injection parameters and producer gas derived from redgram stalk on the performance and emission characteristics of a diesel engine, Alex. Eng. J. 60 (3) (2021) 3133–3142.
[26] K. Mohiuddin, et al., Experimental investigation on the effect of injector hole number on engine performance and particle number emissions in a light-duty diesel engine, Int. J. Engine Res. 22 (8) (2021) 2689–2708.
[27] M. Pandian, S. Sivapirakasam, M. Udayakumar, Investigation on the effect of injection system parameters on performance and emission characteristics of a twin cylinder compression ignition direct injection engine fuelled with pongamia biodiesel–diesel blend using response surface methodology, Appl. Energy 88 (8) (2011) 2663–2676.
[28] A.K. Agarwal, et al., Effect of fuel injection timing and pressure on combustion, emissions and performance characteristics of a single cylinder diesel engine, Fuel 111 (2013) 374–383.
[29] M. Hawi, et al., Effect of injection pressure and ambient density on spray characteristics of diesel and biodiesel surrogate fuels, Fuel 254 (2019), 115674.
[30] P. Kushwaha, S. Ismail, Investigation of the Effects of Oxyhydrogen Gas (HHO) Flow Rate and Injector Penetration on the Performance of a Dual Fuel CI Engine, Indian Chemical Engineer, 2022, pp. 1–13.
[31] D.C. Montgomery, Design and Analysis of Experiments, John wiley & sons, 2017.
[32] P.K. Chaurasiya, et al., Influence of injection timing on performance, combustion and emission characteristics of a diesel engine running on hydrogen-diethyl ether, n-butanol and biodiesel blends, Int. J. Hydrogen Energy 47 (41) (2022) 18182–18193.
[33] U. Rajak, et al., Experimental & predicative analysis of engine characteristics of various biodiesels, Fuel 285 (2021), 119097.
[34] T.N. Verma, et al., Experimental and empirical investigation of a CI engine fuelled with blends of diesel and roselle biodiesel, Sci. Rep. 11 (1) (2021), 18865.
[35] U. Rajak, et al., Effects of Microalgae-Ethanol-Methanol-Diesel Blends on the Spray Characteristics and Emissions of a Diesel Engine, Environment, Development and Sustainability, 2022, pp. 1–22.
[36] L. Ma, et al., Optimization of acidified oil esterification catalyzed by sulfonated cation exchange resin using response surface methodology 98 (2015) 46–53.
[37] S. Dharma, et al., Optimization of biodiesel production process for mixed Jatropha curcas–Ceiba pentandra biodiesel using response surface methodology 115 (2016) 178–190.
[38] V. Silva, A.J.E.C. Rouboa, and Management, Combining a 2-D Multiphase CFD Model with a Response Surface Methodology to Optimize the Gasification of Portuguese Biomasses, vol. 99, 2015, pp. 28–40.
[39] S. Uslu, Optimization of diesel engine operating parameters fueled with palm oil-diesel blend: comparative evaluation between response surface methodology (RSM) and artificial neural network (ANN), Fuel 276 (2020), 117990.
[40] P. Baranitharan, K. Ramesh, R. Sakthivel, Measurement of performance and emission distinctiveness of Aegle marmelos seed cake pyrolysis oil/diesel/TBHQ opus powered in a DI diesel engine using ANN and RSM, Measurement 144 (2019) 366–380.
[41] B. Mohan, et al., Optimization of biodiesel fueled engine to meet emission standards through varying nozzle opening pressure and static injection timing, Appl. Energy 130 (2014) 450–457.
[42] N. Khayum, S. Anbarasu, S. Murugan, Combined effect of fuel injecting timing and nozzle opening pressure of a biogas-biodiesel fuelled diesel engine, Fuel 262 (2020), 116505.
[43] Y. Gülmez, M. Nuran, Effects of nozzle opening pressure and fuel injection timing on engine performance and exhaust emissions of a diesel engine fuelled with marine fuels, Dokuz Eylül Üniversitesi Denizcilik Fakültesi Dergisi 12 (2) (2020) 259–284.
[44] M.E.M. Soudagar, et al., Study of diesel engine characteristics by adding nanosized zinc oxide and diethyl ether additives in Mahua biodiesel–diesel fuel blend, Sci. Rep. 10 (1) (2020), 15326.
[45] S. Molina, et al., Effects of fuel injection parameters on premixed charge compression ignition combustion and emission characteristics in a medium-duty compression ignition diesel engine, Int. J. Engine Res. 22 (2) (2021) 443–455.
[46] P. Sharma, A.K. Sharma, Application of response surface methodology for optimization of fuel injection parameters of a dual fuel engine fuelled with producer gas-biodiesel blends, Energy Sources, Part A Recovery, Util. Environ. Eff. (2021) 1–18.
[47] S. Karthic, et al., An assessment on injection pressure and timing to reduce emissions on diesel engine powered by renewable fuel, J. Clean. Prod. 255 (2020), 120186.
[48] I.S. Mohamed, et al., Optimization of performance and emission characteristics of the CI engine fueled with preheated palm oil in blends with diesel fuel, Sustainability 14 (23) (2022), 15487.
[49] Sathiyamoorthi, R., et al., Optimization of Injection Parameters and Compression Ratio on a Single Cylinder Diesel Engine Fuelled byAzadirachtaIndica (Neem) Biodieselusing Response Surface Methodology (RSM)..
[50] S. Ramalingam, et al., Analysis of optimising injection parameters and EGR for DICI engine performance powered by lemongrass oil using Box–Behnken (RSM) modelling, Int. J. Ambient Energy 43 (1) (2022) 6362–6379.
[51] H. Gürbüz, Y. Şöhret, H. Akçay, Environmental and enviroeconomic assessment of an LPG fueled SI engine at partial load, J. Environ. Manag. 241 (2019) 631–636.
[52] Z. Shi, et al., Effect of injection pressure on the impinging spray and ignition characteristics of the heavy-duty diesel engine under low-temperature conditions, Appl. Energy 262 (2020), 114552.
[53] K. Sivaramakrishnan, P. Ravikumar, Performance optimization of karanja biodiesel engine using taguchi approach and multiple regressions, ARPN J. Eng. Appl. Sci. 7 (4) (2012) 506–516.
[54] T. Shimada, T. Shoji, Y. Takeda, The effect of fuel injection pressure on diesel engine performance, SAE Trans. (1989) 1906–1915.
[55] V. Kamaltdinov, et al., Experimental studies of fuel injection in a diesel engine with an inclined injector, Energies 12 (14) (2019) 2643.
[56] G.M. Tashtoush, M.I. Al-Widyan, A.M. Albatayneh, Factorial analysis of diesel engine performance using different types of biofuels, J. Environ. Manag. 84 (4) (2007) 401–411.
[57] S. Jindal, et al., Experimental investigation of the effect of compression ratio and injection pressure in a direct injection diesel engine running on Jatropha methyl ester, Appl. Therm. Eng. 30 (5) (2010) 442–448.
[58] C. Achebe, et al., Analysis of diesel engine injector nozzle spray characteristics fueled with residual fuel oil, Heliyon 6 (8) (2020), e04637.
[59] H. Chen, et al., Investigation on combustion and emission characteristics of a common rail diesel engine fueled with diesel/n-pentanol/methanol blends, Energy 167 (2019) 297–311.
[60] H. Wang, et al., Study on the performance and emissions of a compression ignition engine fuelled with dimethyl ether, Proc. Inst. Mech. Eng. - Part D J. Automob. Eng. 214 (1) (2000) 101–106.

[61] A. Naveed, Experimental investigation of the effects of fuel injection parameters on diesel engine performance and emissions, J. Eng. Appl. Sci. 36 (1) (2017).
[62] C. Sayin, M. Canakci, Effects of injection timing on the engine performance and exhaust emissions of a dual-fuel diesel engine, Energy Convers. Manag. 50 (1) (2009) 203–213.
[63] T. Ganapathy, R. Gakkhar, K. Murugesan, Influence of injection timing on performance, combustion and emission characteristics of Jatropha biodiesel engine, Appl. Energy 88 (12) (2011) 4376–4386.
[64] J.B. Heywood, Internal Combustion Engine Fundamentals, McGraw-Hill Education, 2018.
[65] H. Yu, et al., Numerical investigation of the effect of two-stage injection strategy on combustion and emission characteristics of a diesel engine, Appl. Energy 227 (2018) 634–642.
[66] X. Tauzia, A. Maiboom, Experimental study of an automotive Diesel engine efficiency when running under stoichiometric conditions, Appl. Energy 105 (2013) 116–124.
[67] M.A. Ijaz Malik, et al., Response surface methodology application on lubricant oil degradation, performance, and emissions in SI engine: a novel optimization of alcoholic fuel blends, Sci. Prog. 106 (1) (2023), 00368504221148342.